Effect of Branching on Polymer Diffusion in Branched Poly(butyl methacrylate) Latex Films

Yuanqin Liu,[†] Walter F. Schroeder,[†] Jeffrey C. Haley,[†] Willie Lau,[‡] and Mitchell A. Winnik*,[†]

Department of Chemistry, University of Toronto, 80 St. George Street, Toronto, Ontario M5S 3H6, and Rohm and Haas Company, 727 Norristown Road, Spring House, Pennsylvania 19477

Received July 8, 2008; Revised Manuscript Received September 6, 2008

ABSTRACT: Fluorescent donor- and acceptor- labeled latex particles comprised of branched poly(butyl methacrylate) (PBMA) were prepared via semicontinuous emulsion polymerization. All latex particles have similar particle size and narrow size distribution. The degrees of branching of the PBMA samples were controlled by adding various amount of bisphenol A dimethacrylate (BPDM) as a branching agent. 1-Dodecanethiol (C_{12}−SH) was used as a chain transfer agent to prevent gel formation and control the molecular weight. The number average molecular weights of all PBMA samples are ca. 45 000 g/mol. The degrees of branching were determined by ^{1}H NMR. Latex films were cast from a 1:1 mixture of donor- and acceptor-labeled latices. The polymer diffusion in the latex films was studied by measuring the energy transfer (ET) from the donor to the acceptor using the time-correlated single photon counting technique. Polymer diffusion rates increased with decreasing values of T_g when the latex films were annealed at 23 °C. After correcting for the effects of T_g, by comparing results at a constant $T - T_g$, ET data show that the PBMA with the highest degree of branching had the highest diffusivity.

Introduction

Latex paints, particularly house paints, are formulated with latex particles consisting of branched polymer. Branching occurs naturally and not intentionally through the choice of monomers used in the synthesis by emulsion polymerization. Coatings referred to as "all-acrylate" are typically copolymers of butyl acrylate (BA) and methyl methacrylate (MMA), whereas the remainder of the market is dominated by latex consisting of copolymers of butyl acrylate and vinyl acetate. In the emulsion copolymerization of these monomers, the butyl acrylate and vinyl acetate propagating radicals have a strong propensity to abstract hydrogens from the polymer backbone, both intramolecularly and intermolecularly, leading respectively to short- and long-chain branches. Lovell's group[1−3] in particular has presented careful studies of these chain-transfer-to-polymer reactions, quantifying the mean number of branch sites per polymer. From the understanding that has been developed, one would predict that the extent of branching in P(BA-MMA) copolymers would increase as the fraction of BA in the monomer mixture was increased. Nevertheless, it remains very difficult to determine the number of long chain branches.

When a dispersion of soft latex particles is applied to a substrate and allowed to dry, it forms a transparent film. This process occurs through three major steps: (i) drying, which brings the particles into contact; (ii) deformation, in which the particles are transformed into space-filling polyhedral cells; (iii) polymer diffusion. The diffusion of polymer molecules across the interfaces between adjacent cells is the step that builds the mechanical properties of the film.[4−16] Long chain branching generally has a profound effect on polymer chain diffusion. In the simplest example, multiarmed star polymer diffusion coefficients typically depend exponentially on star arm length in entangled systems.[17] Near quantitative "dynamic tube dilation" theories account for the combination of arm retraction and constraint release required to predict branched polymer diffusion coefficients. More complicated, branch-on-branch architectures require more complex theories that consider the numbers of segments between branch points and the numbers of branch points. A good overview of the theories for branched polymer dynamics is available.[18] Since branching has an important influence on the polymer diffusion step, it is important that we develop a better understanding of the role of branching in the formation of mechanically coherent films. In a previous study,[19] we examined the rates of polymer diffusion in a series of P(BA-MMA) copolymer latex films and compared the diffusion rates with the linear viscoelastic properties of the film. The results pointed to an increase of branching with increasing BA fraction in the copolymer affecting both the diffusion and rheological properties of the polymer. For example, we found that a higher BA content led to a broader distribution of apparent diffusion coefficients. Since it was not possible to quantify the extent of long-chain branching in those polymers, we began to think about ways in which one could vary the extent of branching in a systematic way in a model latex polymer to study the influence of branching on the polymer diffusion.

As a step in this direction, we turned to a methodology developed by Sherrington and co-workers[20−24] (the "Strathclyde approach") to synthesize gel-free branched polymers by traditional free radical polymerization. In this approach, they carry out their polymerization reactions with a mixture containing both a difunctional cross-linking agent to introduce branch sites and a chain transfer agent to suppress gel formation. In one set of experiments, they showed that this approach could be used in the batch emulsion polymerization of MMA in the presence of but-2-ene-1,4-diacrylate (BDA) as the cross-linking agent and 1-dodecanethiol (C_{12}−SH) as the chain transfer agent.[25] With the correct balance of these two reagents, latex particles containing highly branched soluble PMMA were obtained. In batch polymerization, all of the reactants are added at the beginning of the reaction, and under these circumstances they obtained low molecular weight polymer (M_n < 3300 g/mol) with a very broad molecular weight distribution (MWD).

We tested the idea that higher molecular weight polymers and better molecular weight distributions could be obtained if one carried out the reaction by semicontinuous emulsion polymerization under monomer starved conditions. In this

* Corresponding author.
[†] Department of Chemistry, University of Toronto.
[‡] Rohm and Haas Co.

10.1021/ma801526b CCC: $40.75
Published on Web 11/04/2008

Table 1. Typical Recipe for the Synthesis of Donor-Labeled Branched PBMA Latex

ingredients (g)		first stage	second stage
H_2O		3.0	
SDS		0.030	
Me-β-CD		0.02	
Na_2CO_3		0.05	
KPS		0.06	0.01
monomer pre-emulsion		0.52	16.71
H_2O	10.0		
SDS	0.045		
BMA	4.60		
BPDM	1.18		
PheMMA	0.090		
$C_{12}-SH$	1.31		

approach, one initiates the reaction under batch conditions using a small part of the monomer mixture, and then adds the remaining monomer at a sufficiently slow rate that the monomer is consumed essentially as fast as it is added. As our monomer, we employed butyl methacrylate (BMA). PBMA is a film-forming latex. The polymer produced under these reaction conditions is linear, and the high molecular weight polymer has a glass transition temperature close to 30 °C. Our experiments employed bis-phenol A dimethacrylate (BPDM) as the cross-linking agent and $C_{12}-SH$ as the chain transfer agent. We obtained latex particles uniform in size consisting of polymer with M_n values on the order of 50 000 and $M_w/M_n = 2$. Depending upon the amounts of BPDM and $C_{12}-SH$ used, the polymers obtained ranged from linear or lightly branched to highly branched. In a previous paper,[26] we estimated the entanglement molecular weight of PBMA as $M_e = 34\,000$ from rheological measurements on a well-defined, linear PBMA sample. We also estimated the arm length of the branched polymers that were produced in our synthesis. In all cases, we found that the chain arms were far below the threshold molecular weight to form entanglements; this interpretation was consistent with the linear viscoelastic response of the branched polymers. On this basis, we do not expect that diffusion in our system is described by the theories for the dynamics of entangled branched systems. Instead, we expect that diffusion will be governed primarily by the frictional drag between molecules.

In this paper we show that this methodology is tolerant of dye-containing comonomers. We were able to synthesize donor- and acceptor-labeled PBMA latex particles in which the degree of branching could be controlled independently, while maintaining similar average molecular weights. Through direct nonradiative energy transfer experiments on films formed from these latex, we were able to monitor rates of polymer diffusion as a function of the degree of branching. These experiments lead to the conclusion that for this set of samples, the polymer with the highest degree of branching has the highest diffusivity. We discuss the possible reasons for this result in the sections below.

Experimental Section

Materials. Butyl methacrylate (BMA, Aldrich) was distilled at reduced pressure before use. 4′-Dimethylamino-2-methacryloxy-5-methylbenzophenone (NBenMA) was synthesized as described elsewhere.[27,28] Water was purified by a Milli-Q ion-exchange filtration system. All other chemicals were used as received.

Latex Preparation. Fluorescence dye labeled latex samples were synthesized by semicontinuous emulsion polymerization reactions following a procedure similar to that published previously.[26] For the donor-labeled particles, 1 mol % PheMMA (based on total monomer) was added into the monomer pre-emulsion. For the acceptor-labeled particles, 0.3 mol % NBenMA (based on total monomer) was added into the monomer pre-emulsion. Table 1 shows a typical recipe for the synthesis of donor-labeled branched PBMA.

Characterization of Latex Polymers. A Brookhaven Instruments model BI-90 particle sizer was used to measure the particle sizes and size distributions at 23 °C. The latex solids content was determined by gravimetric analysis. A Brookhaven Instruments model BI-DNDC differential refractometer was used to measure the refractive index increment (dn/dc) at 35 °C. Five concentrations were used for each polymer sample. Polymer molecular weights and molecular weight distributions were measured by gel permeation chromatography (GPC) using a Viscotek liquid chromatograph equipped with a Viscotek model 2501 UV detector and a Viscotek TDA302 triple detector array (TDA). Two Viscotek GMHHR Mixed Bed columns were used with tetrahydrofuran (THF) as the elution solvent at a flow rate of 0.6 mL/min. The GPC column oven temperature was 35 °C and the injection volume was 0.1 mL. The sample was prepared by dissolving the dry polymer in THF, followed by filtering the solution through a 0.2 μm PTFE membrane. The concentration of the THF solution was then determined by gravimetric analysis. The absolute molecular weight was calculated using the dn/dc value. Values of the radius of gyration (R_g) of each polymer were estimated from data obtained from the light scattering detector at low-angle (7°) and at 90°. All data obtained by GPC are listed in Table 2.

Glass transition temperatures (T_g) were determined using a TA Instruments DSC Q100 differential scanning calorimeter.[26] The composition of the polymers were determined by ^{1}H NMR in $CDCl_3$ using a Varian Mercury 300 MHz NMR spectrometer. The UV spectra of NBen-labeled latex samples were measured by a Perkin-Elmer Lambda 6 UV spectrophotometer. A calibration curve was made based on the absorbance at 341 nm of NBenMA solutions in THF. Then the dye concentration in the NBen-labeled polymer was computed based on this calibration curve.

Film Preparation. Latex films for fluorescence decay measurements were prepared from 1:1 particle mixtures of the donor- and acceptor-labeled dispersions. Several drops of a latex dispersion (about 20 wt % solids content) were spread on a small quartz plate (20 × 8 mm). The film was allowed to dry uncovered at 4 °C until visually transparent. It took about 2 h for a film to dry. The films prepared in this way have a thickness of ca. 40 μm.

Solvent-cast films were prepared from the same latex mixture. A latex film was allowed to dry at 23 °C overnight, and the dry film was dissolved in a minimum amount of THF. The solution was recast onto a small quartz plate and allowed to dry at room temperature for 24 h.

Film Annealing and Fluorescence Decay Measurements. *Film Annealing.* Latex films on quartz plates were placed directly on a high mass (2 cm thick) aluminum plate in an oven preheated to the annealing temperature and then annealed for various periods of time. Under these conditions, we estimate that it takes less than 1 min for the film to reach the preset oven temperature. The annealed films were taken out of the oven and placed directly on another high mass aluminum plate at 4 °C for 2 min before carrying out fluorescence decay measurements.

Fluorescence Decay Measurements. Fluorescence decay profiles[29] of the films at 23 °C were recorded using a nanosecond Time-Correlated Single Photon Counting System from IBH. Each film was placed in a quartz tube and excited with a NanoLED (λ_{ex} = 296 nm). An emission monochromator (350 ± 16 nm) was used to minimize the amount of scattered light from the sample entering the detector. Data were collected until 5000 counts were accumulated in the maximum channel. The instrumental response function was obtained by using a degassed *p*-terphenyl solution (0.96 ns lifetime) as a mimic standard.[30]

Data Analysis. For all the latex polymers examined in this work, the donor (Phe) decay profile in films free of acceptors was exponential with a lifetime $\tau_D = 44.3$ ns. For films containing both donor and acceptor chromophores, the fluorescence-decay profiles became nonexponential. The shape of the curve depends upon the details of the donor−acceptor pair distribution. In a system containing uniformly distributed donor and acceptors in three dimensions in the absence of diffusion, the donor fluorescence

Table 2. Characteristics of the Latex Polymers and Particles

latex samples[a]	mole feed ratio BMA/BPDM/C_{12}−SH	mole ratio by ^{1}H NMR BMA/BPDM	d*n*/d*c*	molecular weight[b] (g/mol) M_n	M_w	M_w/M_n	R_g (nm)	T_g (°C)	particle size *d* (nm)	*poly*[c]	solids content (%)
LR-PBMA^D	100/0/1	100/0	0.072	50 000	78 000	1.6	3.0	24	132	0.040	18.9
LR-PBMA^A	100/0/1	100/0	0.071	53 000	77 000	1.5	3.1	25	102	0.060	20.8
LB-PBMA^D	100/1/2	100/1.3	0.075	39 000	67 000	1.7	2.8	18	131	0.041	19.8
LB-PBMA^A	100/1/2	100/1.6	0.076	49 000	77 000	1.6	2.8	22	105	0.026	23.7
MB-PBMA^D	100/5/10	100/6.2	0.076	45 000	81 000	1.8	2.7	2	139	0.016	19.2
MB-PBMA^A	100/5/10	100/5.3	0.080	41 000	65 000	1.6	2.5	5	137	0.036	20.0
HB-PBMA^D	100/10/20	100/9.9	0.087	41 000	78 000	1.9	2.1	2	100	0.028	19.3
HB-PBMA^A	100/10/20	100/9.4	0.084	47 000	79 000	1.7	2.2	5	138	0.033	22.3

[a] The type of fluorescent dye is indicated by the superscript "D" or "A", which represents "donor" or "acceptor", respectively. The degree of branching is indicated by LR (linear), LB (low-branched), MB (medium-branched), and HB (highly branched) according to the molar fraction of BPDM. [b] Absolute molecular weights were measured by GPC using a Viscotek TDA302 triple detector array. [c] Polydispersity (*poly*) in terms of the cumulants of the logarithm of the measured correlation function. It is a measure of the width of the particle size distribution, taking values close to zero (0.000 to 0.020) for nearly monodisperse samples, and small (0.020 to 0.080) for narrow size distributions.

intensity decay $I_D(t')$ following instantaneous excitation is described by the Förster equation,[31]

$$I_D(t') = A \exp[-t'/\tau_D - P(t'/\tau_D)^{1/2}] \quad (1)$$

where

$$P = \frac{4}{3}\pi^{3/2}\left(\frac{3}{2}\langle\kappa^2\rangle\right)^{1/2} N_A R_0^3 [\mathrm{A}] \quad (2)$$

Here, P is proportional to the acceptor (quencher) concentration [A]. R_0 is the critical Förster radius for energy transfer, which for the Phe/NBen pair takes a value of 2.51 ± 0.04 nm.[19] N_A is Avogadro's number. The orientation factor $\langle\kappa^2\rangle$ describes the average orientation of dipoles of donor and acceptor molecules. For a random distribution of immobile chromophores in three-dimensions, $\langle\kappa^2\rangle$ is replaced by $\langle\kappa\rangle^2 = 0.476$, a situation typical of dyes in polymer matrices.[28,32]

The quantum efficiency of energy transfer $\Phi_{ET}(t)$ is defined by the middle term in the following expression

$$\Phi_{ET}(t) = 1 - \frac{\int_0^\infty I_D(t', t)\, \mathrm{d}t'}{\int_0^\infty I_D^0(t')\, \mathrm{d}t'} = 1 - \frac{\mathrm{area}(t)}{\tau_D} \quad (3)$$

where $I_D^0(t')$ is the decay curve of donor fluorescence intensity in the donor-only film. Because the unquenched donor decay profile was exponential in each sample, its integral is equal to the unquenched donor lifetime τ_D. Here t is the annealing time after film preparation; t' is the fluorescence decay time; and area(t) refers to the normalized area under the fluorescence decay curve of a film annealed for time t.

To obtain the area for each decay profile, we fit each decay curve to the empirical eq 4 and then evaluate the integral analytically from the magnitude of the fitting parameters, A_1, A_2, and p.[26−28]

$$I_D(t', t) = A_1 \exp[-t'/\tau_D - p(t'/\tau_D)^{1/2}] + A_2 \exp(-t'/\tau_D) \quad (4)$$

The fraction of mixing f_m is an important parameter measuring the extent of growth of Φ_{ET} due to polymer diffusion, and is defined in such a way that it corrects for the energy transfer efficiency in the nascent films. Values of f_m are calculated from fluorescence decay data using the following equation

$$f_m(t) = \frac{\Phi_{ET}(t) - \Phi_{ET}(0)}{\Phi_{ET}(\infty) - \Phi_{ET}(0)} \quad (5)$$

where, in principle, the numerator represents the change in energy transfer efficiency between the freshly prepared film and that annealed for time t, and the denominator describes the difference in energy transfer efficiency between the initial and the fully mixed films. Because some polymer diffusion can occur during sample drying, we fitted data to eq 5 using a value of $\Phi_{ET}(0) = 0.07$, which corresponds to films formed from latex particles of the size employed here, which achieve intimate contact upon drying,[33] but for which no polymer diffusion takes place.[34]

Rheological Measurements. The linear viscoelastic response of the PBMA samples was studied at several temperatures above T_g with a Rheometrics RAA instrument in the oscillatory shear mode employing parallel plates (25 mm diameter). The frequency was scanned between 0.01 and 100 rad/s at a constant temperature. Strain sweeps were employed to ensure that all measurements were made in the linear viscoelastic regime. The range of temperatures studied was selected to be as close as possible to the range of temperatures used in the energy transfer experiments performed on these materials. However, the lowest temperatures used are limited by the sample modulus at temperatures close to T_g. The samples for rheological measurements were prepared as described in our previous paper.[26]

Results and Discussion

Synthesis of Dye-Labeled Branched PBMA Latex Particles. The protocol employed here for the synthesis of dye-labeled latex particles follows the strategy which we reported recently.[26] BPDM served as the branching agent, and C_{12}−SH was used as the chain transfer agent. By generating seed particles *in situ* using a small fraction (typically 3 wt %) of the monomer pre-emulsion in a batch reaction, we avoided the contribution of small amounts of high molecular weight linear polymer typical of PBMA seed particles. The *in situ* seeding process also helped to achieve a homogeneous distribution of the dye comonomer in latex particles. A typical recipe for the synthesis of Phe-labeled branched PBMA latex is presented in Table 1. We added 1 mol % (based on total monomer) of the fluorescent donor dye comonomer (PheMMA) into the monomer pre-emulsion. To prepare acceptor-labeled PBMA latex, 0.3 mol % of NBenMA was used instead of PheMMA. A phase transfer agent (Me-β-CD) was also added to enhance the transport of C_{12}−SH and BPDM from the monomer droplets through the aqueous phase to the growing particles during the polymerization.[35]

By varying the concentration of BPDM, we synthesized matched pairs of donor- and acceptor- labeled latex particles with different degrees of branching. In our notation, "LR" refers to linear polymer, synthesized without BPDM. The "low-branched" (LB) polymer was synthesized with 1 mol % BPDM (based upon total monomer); the "medium-branched" MB polymer with 5 mol % BPDM; and the "highly branched" (HB) polymer with 10 mol % BPDM. The type of fluorescent dye is indicated by a superscript "D" or "A", which represents "donor" or "acceptor", respectively. For example, the Phe-labeled middle-branched PBMA sample is written as MB-PBMA^D.

To obtain meaningful absolute molecular weights, we carried out gel permeation chromatography (GPC) measurements using an instrument equipped with triple detector array (TDA/GPC) in conjunction with d*n*/d*c* values determined independently by differential refractometry. We observed that the values of d*n*/d*c* increased as the fraction of BPDM in the polymer increased

Table 3. Estimation of the Chain Structure of the Different Branched Latices

latex samples	N_{BMA}[a]	N_{BPDM}[b]	N_{end}[c]	n_{BMA}[d]
LR-PBMA^D	353	0	2	353
LR-PBMA^A	371	0	2	371
LB-PBMA^D	266	3	8	23
LB-PBMA^A	328	5	12	20
MB-PBMA^D	275	17	36	5
MB-PBMA^A	253	13	28	6
HB-PBMA^D	231	23	48	3
HB-PBMA^A	265	25	52	3

[a] Average number of BMA units per chain. [b] Average number of BPDM units per chain. [c] Average number of end groups per chain. [d] Average number of BMA units between two branching points.

(Table 2), but were independent of the type of labeled dye. The data in Table 2 show three important features. First, all samples have relatively high molecular weights. M_n values are greater than 39,000 g/mol, and M_w values are greater than 67,000 g/mol. Second, the molecular weight distribution is narrower than that typically obtained by traditional semicontinuous emulsion polymerization. Calculated values of M_w/M_n are less than 1.9. While the light scattering detector provides reliable values of M_w, it can underestimate M_n. Thus we consider these M_w/M_n values to be indistinguishable from 2.0. Third, the molecular weights are similar for all samples independent of the degree of branching and of the type of dye comonomer. These results demonstrate our ability to control the molecular weight and to label the branched polymers.

The degree of branching was controlled by tuning the feed ratio of BMA/BPDM. The mole ratios of BMA/BPDM incorporated into the latex polymers were calculated from ^{1}H NMR spectra (Table 2) as described in ref 26. The experimental values are very close to the feed ratios for all degrees of branching. Combining the BMA/BPDM ratios with the M_n values, we estimated the chain structures of the dye-labeled branched PBMA samples (Table 3). N_{BMA} and N_{BPDM} represent the average number of BMA units and BPDM units per polymer chain. Since each BPDM unit introduces two more end groups into the chain, the average number of end groups per chain (N_{end}) is given by the equation

$$N_{end} = 2 + 2N_{BPDM} \quad (6)$$

In addition each BPDM divides the chain into three segments between branch or end points. This average number of BMA units between two adjacent branch points (n_{BMA}) is given by the expression:

$$n_{BMA} = N_{BMA}/(1 + 3N_{BPDM}) \quad (7)$$

The calculated average values of N_{BMA}, N_{BPDM}, N_{end}, and n_{BMA} are collected in Table 3. One can see that the N_{end} values increase significantly with N_{BPDM}, as expected.

The results also show that the glass transition temperature (T_g) decreases as N_{end} increases. For example, LR-PBMA^D, which is linear, has a T_g value of 24 °C. In contrast, the T_g of HB-PBMA^D is only 2 °C. This decrease in T_g can be understood from the increment in free volume associated with the higher average number of end groups per chain and from the larger content of oligomer in this sample. There is an indication of this oligomer content in the GPC elution profile shown in Figure 1. Increased branching at constant molar mass led to a more compact polymer structure in solution and to a pronounced decrease in the glass transition temperature in the bulk state. Information about polymer dimensions in solution is available from R_g values determined from the GPC light scattering detectors (Table 2) and from the GPC elution sequence as shown in Figure 1.

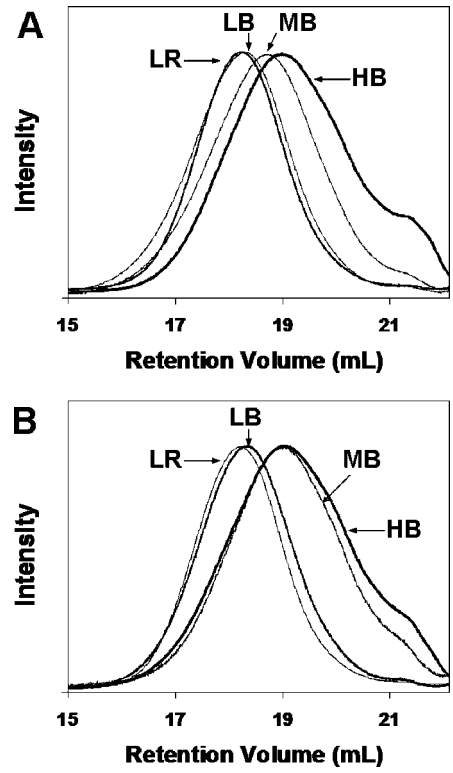

Figure 1. GPC traces (RI) for (A) acceptor- and (B) donor-labeled PBMA samples.

These results show that by the semicontinuous emulsion polymerization, we were able to control the extent of branching without loss of control over particle size and size distribution. As shown in Table 2, the average diameters for all the latex particles were in the range of 100 to 140 nm. The size distributions are very narrow in all cases. The other feature of semicontinuous emulsion polymerization under monomer starved conditions is that it ensures the random distribution of dye comonomers in the polymer chains. Evidence for the uniform dye distribution is provided by the GPC traces in Figure 2, where the RI detector monitors elution of the polymer, whereas the UV signal responses to the presence of the chromophore. The close overlap of the UV and RI traces indicates a close to random distribution of the chromophores in the polymer chains.

Polymer Diffusion in Branched PBMA Latex Films at Same Temperature. In this section we analyze the effect of branching on polymer diffusion rates in branched PBMA latex films annealed at the same temperature. In these experiments we monitored the increase in energy transfer efficiency of branched latex films, annealed for specified times at a given temperature. Before we compare Φ_{ET} data to evaluate changes in polymer diffusion, it is necessary to examine if samples with different branching degree have similar limiting values of energy transfer efficiency in the state of full mixing ($\Phi_{ET}(\infty)$). To obtain samples to serve as a model for $\Phi_{ET}(\infty)$, we dissolved the labeled latex mixture in an organic solvent. In solution, one expects full mixing of the donor- and acceptor-labeled latex polymers. A film cast from the solution is then a good model for the determination of $\Phi_{ET}(\infty)$.

A dry latex film containing a 1:1 (w/w) mixture of donor- and acceptor-labeled linear or branched polymers was dissolved in a minimum amount of THF. This solution was recast onto a quartz plate and allowed to dry at room temperature for 24 h. Then, from the fluorescence decay profiles we obtained the limiting values of energy transfer efficiency corresponding to the state of full mixing, under the assumption that the two

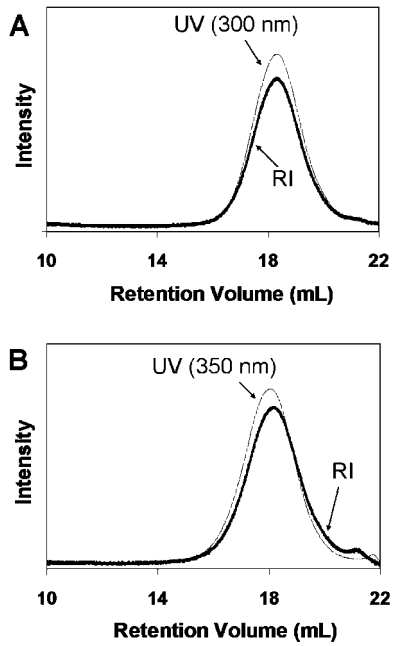

Figure 2. GPC traces of (A) LB-PBMA^{D} and (B) LB-PBMA^{A}. The UV and RI traces overlap, which indicates a nearly random distribution of dye comonomers in the polymer chains.

labeled polymers mix completely when dissolved in that solvent and that they do not demix upon drying. The values obtained for the different samples, listed in Table 4 as $\Phi_{ET}(\infty)^{exp}$, are in the range of 0.36 − 0.40. Since the differences among the $\Phi_{ET}(\infty)^{exp}$ values for the different branching degree are similar to the experimental uncertainty of quantum efficiency measurements (ca. ± 0.02), these limiting values can be considered identical within experimental error.

To confirm that these $\Phi_{ET}(\infty)^{exp}$ values truly represent fully randomized donor- and acceptor-labeled branched polymer mixtures, we calculated the limiting values of energy transfer efficiency using the Förster model given by eqs 1 and 2. To measure the acceptor concentration in each latex film sample, a calibration curve was constructed by measuring the UV absorbance at 340 nm of a series of acceptor standard solutions (Figure S1 in Supporting Information). The UV absorbance for each film was then measured at the same wavelength and the acceptor concentration was calculated from the calibration curve. The obtained acceptor concentrations in the polymer film range from 10.7 to 12.1 mmol/L (acceptor/polymer film) and are listed in Table 4. These concentration values were used (eq 2) to calculate the values of Förster fitting parameter P corresponding to each branched latex film. This parameter accounts for the influence of energy transfer in a system containing uniformly distributed donor and acceptors in three dimensions. Then, limiting values of energy transfer efficiency were calculated ($\Phi_{ET}(\infty)^{cal}$) using eq 1 and eq 3, and considering the pre-exponential factor in the Förster equation as $A = 1$. Table 4 lists the obtained $\Phi_{ET}(\infty)^{cal}$ values for the different branched latex mixtures. One can see that these results are in good agreement with those obtained experimentally from THF-cast films, indicating that the $\Phi_{ET}(\infty)^{exp}$ values truly correspond to the state of full mixing at molecular level of donor- and acceptor-labeled branched polymers.

To study polymer diffusion rates, latex films with different degrees of branching were cast from 1:1 D/A mixtures. All latex films were clear and crack free. These films were annealed at different temperatures, and ET measurements were carried out at various annealing times. To compare the polymer diffusion rates in the branched PBMA latex films, we plotted the Φ_{ET} values as a function of annealing time at common annealing temperatures in Figure 3. Figure 3(A) shows that at 23 °C, the HB-PBMA$^{D/A}$ and MB-PBMA$^{D/A}$ films undergo a significant extent of diffusion on the time scale of hours. In contrast, the LB-PBMA$^{D/A}$ and LR-PBMA$^{D/A}$ films show a much smaller increase of Φ_{ET} values for the same time scale. The $\Phi_{ET}(0)$ value of 0.20 for the HB-PBMA$^{D/A}$ sample indicates that a significant amount of polymer diffusion occurred during sample drying. One conclusion that can be drawn from these data is that the polymer diffusion rate at 23 °C increases as the T_g of the sample decreases.

The Φ_{ET} values of all films are plotted as a function of the annealing time at 45 °C in Figure 3B. It can be observed that polymer diffusion rates in the LB-PBMA$^{D/A}$ and LR-PBMA$^{D/A}$ films significantly increased with respect to the films annealed at 25 °C (Figure 3A). Their Φ_{ET} values approached 0.30 over three hours. Upon annealing at 70 °C, all latex film samples exhibited a behavior analogous to that of the low T_g sample: rapid diffusion at early times, followed by a leveling off at a Φ_{ET} value close to the corresponding $\Phi_{ET}(\infty)^{exp}$ value. In Figure 4, we plot the values of fraction of mixing f_m as a function of annealing time for the branched latex films at the different annealing temperatures. These f_m values were calculated from eq 5, using the corresponding $\Phi_{ET}(\infty)^{exp}$ value for each labeled latex mixture given in Table 4. One can see that each f_m curve presents similar features to the corresponding Φ_{ET} curve in Figure 3.

To compare polymer diffusion rates quantitatively at different temperatures, we calculated *apparent* mean diffusion coefficients D_{app} that characterize the diffusive transport of the labeled-polymer chains in the latex film. We computed these values by fitting the f_m data to a Fickian diffusion model for spherical geometry (the procedure is described in Supporting Information). These D_{app} values are not the true center-of-mass diffusion constants for the polymers; however, our experience has shown that D_{app} provides a realistic measure of the changes in polymer diffusion rates.[13−16,27,28] Using simulations,[19,34] we have shown that for values of $f_m \leq 0.7$, D_{app} values are proportional to, but larger than the center-of-mass diffusion coefficients of the polymer molecules. D_{app} values for all samples were calculated as a function of f_m at each temperature (Figure S2 in Supporting Information). The decrease in D_{app} values at increasing values of f_m are an indication that slower diffusing species make increasingly large contributions to the growth in energy transfer. As $f_m \rightarrow 1$, however, Φ_{ET} approaches its maximum value, and the ET experiment loses sensitivity to further polymer diffusion.

To compare the D_{app} values, we created D_{app} master curves for all samples by vertically shifting the data points at 45 and 70 °C to overlap the data points at 23 °C (Figure 5). The most impressive feature in Figure 5 is that the master curves of the HB-PBMA$^{D/A}$ and the MB-PBMA$^{D/A}$ films are at least 2 orders of magnitude higher than those of the LB-PBMA$^{D/A}$ and LR-PBMA$^{D/A}$ films. For the same value of f_m, the sample with a lower T_g has higher D_{app} value. For example, at $f_m = 0.84$, the plot shows a value of $D_{app} = 2.5 \times 10^{-1}$ nm^2/s for the HB-PBMA$^{D/A}$ film, 2.8×10^{-2} nm^2/s for the MB-PBMA$^{D/A}$ film, 1.5×10^{-4} nm^2/s for the LB-PBMA$^{D/A}$ film, and 1.7×10^{-6} nm^2/s for the LR-PBMA$^{D/A}$ film.[36] Since the T_g has an important effect upon the diffusive capability of polymer chains, a proper analysis of the effect of branching on polymer diffusion should involve a correction for the different T_g values of the branched samples. We develop this analysis in the next section.

Polymer Diffusion in Branched PBMA Latex Films at T_g + 20 °C. Because of the significant T_g effect on polymer diffusion, it is difficult to quantify the influence of branching on polymer diffusion from the previous analysis of the ET data. Models of polymer rheology suggest that polymers of similar composition (i.e., with similar friction coefficients) and similar

Table 4. Limiting Values of Energy Transfer Efficiency for the Different Labeled Latex Mixtures

D/A (1/1) labeled latex mixture	C_{Nben} [μmol/g (NBen /polymer)]	C_{Nben} [mmol/L (NBen/polymer film)]	$[\Phi_{ET}(\infty)^{exp}]^a$	$[\Phi_{ET}(\infty)^{cal}]^b$
LR-PBMA$^{D/A}$	11.1	11.7	0.40	0.43
LB-PBMA$^{D/A}$	10.5	11.0	0.38	0.42
MB-PBMA$^{D/A}$	10.2	10.7	0.36	0.41
HB-PBMA$^{D/A}$	11.5	12.1	0.39	0.44

[a] Limiting values of Φ_{ET} obtained from fluorescence decays for THF-cast films. [b] Limiting values of Φ_{ET} calculated from the Förster equation (eq 1) using $R_0 = 2.51$ nm.[19]

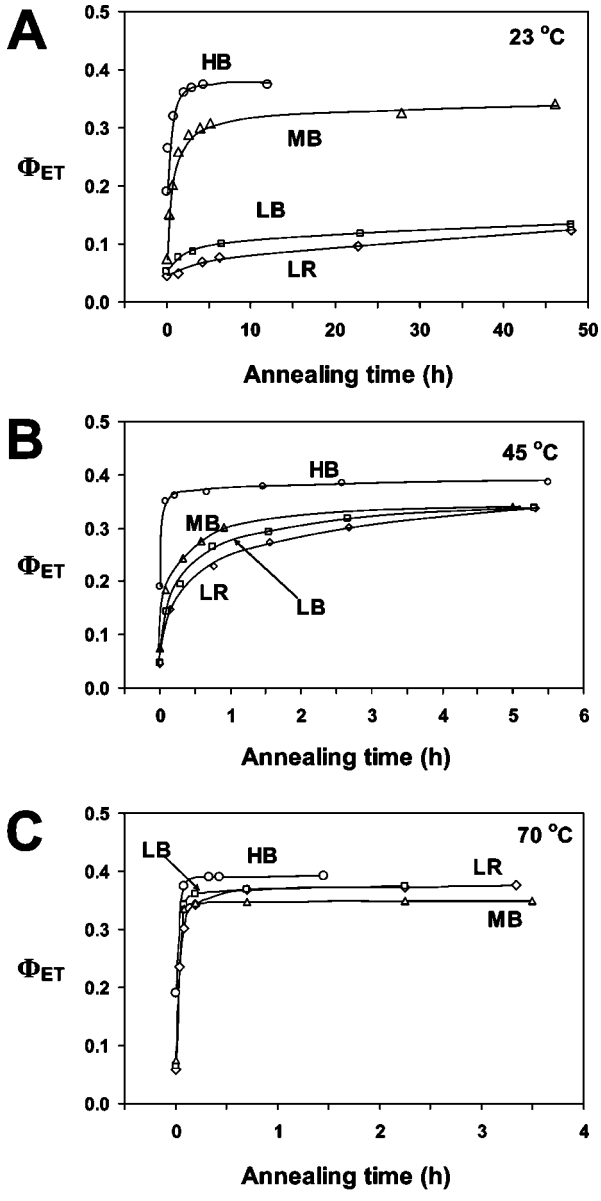

Figure 3. Plot of the Φ_{ET} for films formed from D/A labeled latex mixtures annealed for various periods of time at (A) 23 °C, (B) 45 °C, and (C) 70 °C. Key: (○) HB-PBMA$^{D/A}$, (△) MB-PBMA$^{D/A}$, (□) LB-PBMA$^{D/A}$, and (◇) LR-PBMA$^{D/A}$. All solid lines are guide lines for the eye.

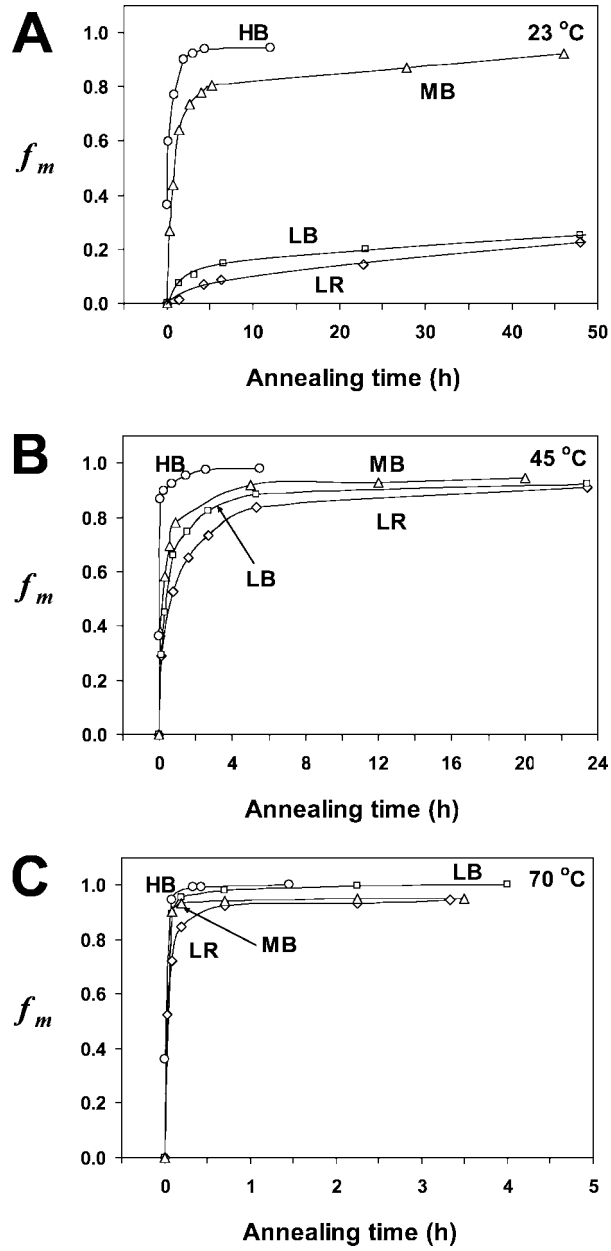

Figure 4. Plot of the f_m for films formed from D/A labeled latex mixtures annealed for various periods of time at (A) 23 °C, (B) 45 °C and (C) 70 °C. Key: (○) HB-PBMA$^{D/A}$, (△) MB-PBMA$^{D/A}$, (□) LB-PBMA$^{D/A}$, and (◇) LR-PBMA$^{D/A}$. All solid lines are guide lines for the eye.

molecular weights, but different T_g values, should have similar mobility when they are annealed at the same constant temperature above their T_g's.[37] To eliminate the effect of T_g, latex films were prepared as described previously and each annealed at T_g + 20 °C. ET measurements were then carried out on samples cooled to room temperature to stop polymer diffusion during the measurement.

In Figure 6A, the calculated f_m values are plotted as a function of annealing time for the films annealed at (T_g + 20) °C. The plot shows that f_m increases rapidly at the early stages, followed by a slower increase at longer annealing times. In the early stage, the sample with a higher degree of branching has a higher f_m value. For example, the f_m value after 1 h annealing is 0.65 for the HB-PBMA$^{D/A}$ film, 0.55 for the MB-PBMA$^{D/A}$ film, and 0.19 for the LB-PBMA$^{D/A}$ film. After annealing for one day, the three films showed similar values of f_m.

To quantify the effect of branching on the distribution of diffusion rates in the system, apparent mean diffusion coefficients

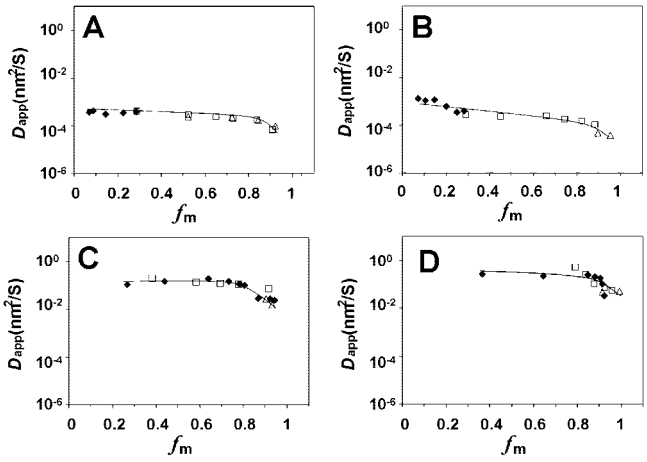

Figure 5. Master curves of D_{app} for (A) LR-PBMA$^{D/A}$, (B) LB-PBMA$^{D/A}$, (C) MB-PBMA$^{D/A}$, and (D) HB-PBMA$^{D/A}$. Here, 23 °C was used as the reference temperature. The apparent precipitous decrease in D_{app} values at values of $f_m \rightarrow 1$ may not be real, since the energy transfer methodology loses its sensitivity as polymers approach the fully mixed state, and the acceptor concentrations in the films become uniform. All solid lines are guide lines for the eye.

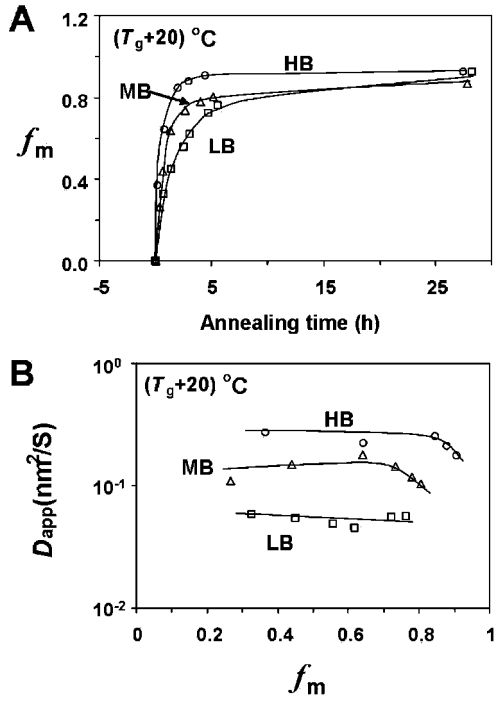

Figure 6. (A) Plot of f_m for films annealed at (T_g +20) °C. (B) Plot of D_{app} over f_m at (T_g +20) °C. Key: (○) HB-PBMA$^{D/A}$, (△) MB-PBMA$^{D/A}$, and (□) LB-PBMA$^{D/A}$. All solid lines are guide lines.

D_{app} were calculated by fitting the f_m data to a spherical diffusion model that satisfies Fick's second law of diffusion (as described in the Supporting Information). We then plotted D_{app} as a function of f_m in Figure 6B. It can be observed that the branching structure had significant influence upon D_{app}. The figure shows that at $f_m < 0.90$, the samples with a higher degree of branching had greater D_{app} values. From all these experiments, we conclude that an increase in the branching degree of PBMA latex enhances the polymer diffusion rate during film formation process.

In Figure 6B, the D_{app} plot indicates that the degree of branching has a significant effect on polymer diffusion rate. One might normally expect that increasing the degree of branching would retard the polymer diffusion rate. However, our experimental data show the opposite result. We believe that the main reason for this behavior is related to the architectures of the branched PBMA samples. As indicated in Table 3, the branched PBMA samples have short branches. For example, each LB-PBMA$^{D/A}$ chain contains branches with an average length of ca. 20 BMA units. The more branched PBMA samples are composed of even shorter branches. The MB-PBMA$^{D/A}$ sample contains ca. 6 BMA units per branch, and each HB-PBMA$^{D/A}$ branch has an average length of ca. 3 BMA units. These branches are much too short to form entanglements between polymer chains.[26] The lack of entanglement in these branched PBMA samples has been established by detailed linear rheology measurements (Figure S3 in Supporting Information). It is the formation of entanglements with different polymer chains that slows down the polymer diffusion in branched samples. Thus it is not surprising that the HB-PBMA$^{D/A}$ sample does not have a slower diffusion rate than the LB-PBMA$^{D/A}$ sample. Furthermore, instead of forming entanglements, the short branches constrain the polymer chains to form a compact structure. This result is reflected in values of R_g obtained in the TDA/GPC measurements (Table 2). For example, the LB-PBMA$^{D/A}$ sample has a R_g value of 2.8 nm while the HB-PBMA$^{D/A}$ sample has a R_g value of 2.1 nm. Because the magnitude of R_g is related to that of the hydrodynamic radius R_h, and molecules with smaller R_h diffuse faster than those with greater R_h, the decrease in R_g can explain why the HB-PBMA$^{D/A}$ sample diffuses faster than the other samples.

Summary

We synthesized four sets of latex particles comprised of PBMA with various degree of branching. To carry out energy transfer studies of polymer diffusion, donor and acceptor dyes were incorporated in the PBMA particles, respectively. All branched polymers have similar molecular weights and are free of gel. The latex particles have a similar particle size and a narrow size distribution. The ET technique was applied to study the effect of branching on the rate of polymer diffusion in the PBMA latex films. Comparison of the diffusion data indicates that T_g has a significant effect on polymer diffusion when the films were annealed at 23 °C. By examining films annealed at T_g + 20 °C, we could correct for the influence of T_g. In this way, we found that the diffusion rate of branched PBMA increases as the degree of branching increases. The more highly branched polymers have more compact structures.

Acknowledgment. The authors thank Rohm & Haas, Rohm and Haas Canada, and NSERC Canada for their support of this research. Y. L. thanks the Province of Ontario for an Ontario Graduate Scholarship in Science and Technology (OGSST) scholarship.

Supporting Information Available: Figures showing the calibration curve for NBen, plots of log D_{app} vs f_m for all samples, and plots of master curves of G' and G'' for all samples, and text discussing the calculation of apparent diffusion coefficients. This material is available free of charge via the Internet at http://pubs.acs.org.

References and Notes

(1) Ahmad, N. M.; Heatley, F.; Lovell, P. A. *Macromolecules* **1998**, *31*, 2822–2827.
(2) Britton, D.; Heatley, F.; Lovell, P. A. *Macromolecules* **1998**, *31*, 2828–2837.
(3) Heatley, F.; Lovell, P. A.; Yamashita, T. *Macromolecules* **2001**, *34*, 7636–7641.
(4) Dillon, R. E.; Metheson, L. A.; Bradford, E. B. *J. Colloid Sci.* **1951**, *6*, 108.

(5) Henson, W. A.; Taber, D. A.; Bradford, E. B. *Ind. Eng. Chem.* **1953**, *45*, 735.
(6) Brown, G. L. *J. Polym. Sci.* **1956**, *22*, 423.
(7) Hwa, C. H. J. *J. Polym. Sci., Part A* **1964**, *2*, 785–796.
(8) Myers, R. R.; Schultz, K. R. *J. Polym. Sci., Part A* **1964**, *8*, 755–764.
(9) Sheetz, D. P. *J. Appl. Polym. Sci.* **1965**, *9*, 3759–3773.
(10) Hahn, K.; Ley, G.; Schuller, H.; Oberthür, R. *Colloid Polym. Sci.* **1986**, *264*, 1092–1096.
(11) Hahn, K.; Ley, G.; Oberthür, R. *Colloid Polym. Sci.* **1988**, *266*, 631–639.
(12) Chevalier, Y.; Pichot, C.; Graillat, C.; Joanicot, M.; Wong, K.; Maquet, J.; Lindner, P.; Cabane, B. *Colloid Polym. Sci.* **1992**, *270*, 806–821.
(13) Keddie, J. L. *Mater. Sci. Eng.* **1997**, *21*, 101–170.
(14) Wu, J.; Oh, J. K.; Yang, J.; Winnik, M. A.; Farwaha, R.; Rademacher, J. *Macromolecules* **2003**, *36*, 8139–8147.
(15) Oh, J. K.; Tomba, P.; Ye, X.; Eley, R.; Rademacher, J.; Farwaha, R.; Mitchell, M. A. *Macromolecules* **2003**, *36*, 5804–5814.
(16) Oh, J. K.; Wu, J.; Winnik, M. A.; Craun, G. P.; Rademacher, J.; Farwaha, R. *J. Polym. Sci., Part A: Polym. Chem.* **2002**, *40*, 3001–3011.
(17) Klein, J.; Fletcher, D.; Fetters, L. J. *Nature* **1983**, *304*, 526–527.
(18) McLeish, T. C. B. *Adv. Phys.* **2002**, *51*, 1379–1527.
(19) Liu, Y.; Haley, J. C.; Deng, K.; Lau, W.; Winnik, M. A. *Macromolecules* **2007**, *40*, 6422–6431.
(20) O'Brien, N.; McKee, A.; Sherrington, D. C. *Polym. Commun.* **2000**, *41*, 6027–6031.
(21) Costello, P. A.; Martin, I. K.; Slark, A. T.; Sherrington, D. C.; Titterton, A. *Polymer* **2002**, *43*, 245–254.
(22) Isaure, F.; Cormack, P. A. G.; Sherrington, D. C. *J. Mater. Chem.* **2003**, *13*, 2701–2710.
(23) Slark, A. T.; Sherrington, D. C.; Titterton, A.; Martin, I. K. *J. Mater. Chem.* **2003**, *13*, 2711–2720.
(24) Isaure, F.; Cormack, P. A. G.; Sherrington, D. C. *Macromolecules* **2004**, *37*, 2096–2105.
(25) Baudry, R.; Sherrington, D. C. *Macromolecules* **2006**, *39*, 1455–1460.
(26) Liu, Y.; Haley, J. C.; Deng, K.; Lau, W.; Winnik, M. A. *Macromolecules* **2008**, *41*, 4220–4225.
(27) Oh, J. K.; Wu, J.; Winnik, M. A.; Craun, G. P.; Rademacher, J.; Farwaha, R. *J. Polym. Sci., Part A: Polym. Chem.* **2002**, *40*, 1594–1607.
(28) Ohpr, J. K.; Wu, J.; Winnik, M. A.; Craun, Gary, P.; Rademacher, J.; Farwaha, R. *J. Polym. Sci., Part A: Polym. Chem.* **2002**, *40*, 3001–3011.
(29) O'Connor, D. V.; Phillips, D. *Time-Correlated Single Photon Counting*; Academic Press, New York, 1984.
(30) James, D. R.; Demmer, D. R. M.; Verrall, R. E.; Steer, R. P. *Rev. Sci. Instrum.* **1983**, *54*, 1121–1130.
(31) Bartels, C. R.; Buckley, C.; Graessley, W. W. *Macromolecules* **1984**, *17*, 2702–2708.
(32) Baumann, J.; Fayer, M. D. *J. Chem. Phys.* **1986**, *85*, 4087–4107.
(33) (a) Wool, R. P.; O'Connor, K. M. *J. Appl. Phys.* **1981**, *52*, 5953. (b) Kim, Y. H.; Wool, R. P. *Macromolecules* **1983**, *16*, 1115.
(34) Farinha, J. P. S.; Martinho, J. M. G.; Yekta, A.; Winnik, M. A. *"Macromolecules* **1995**, *28*, 6084–6088.
(35) Lau, W. Method for forming polymers. U.S. Patent 5,760,129, June 2, **1998**.
(36) Note that $D_{app} = 0.1$ nm^2/s $= 10-15$ cm^2/s.
(37) Ferry, J. D. *Viscoelastic Properties of Polymers*; Wiley: New York, 1980.

MA801526B